Smart Materials and Structures

Smart passive system based on magnetorheological damper

To cite this article: Sang-Won Cho *et al* 2005 *Smart Mater. Struct.* **14** 707

View the article online for updates and enhancements.

You may also like

- The development of an outer multi-pole magneto-rheological damper with high dynamic range of damping force
Shaogang Liu, Lifeng Feng, Dan Zhao et al.
- Design and experiments of a novel magneto-rheological damper featuring bifold flow mode
Kyongsol Kim, Zhaobo Chen, Dong Yu et al.
- MR damper based implementation of nonlinear damping for a pitch plane suspension system
H Laalej, Z Q Lang, B Sapinski et al.

This content was downloaded from IP address 14.139.194.106 on 07/09/2023 at 20:08

INSTITUTE OF PHYSICS PUBLISHING SMART MATERIALS AND STRUCTURES
Smart Mater. Struct. **14** (2005) 707–714 doi:10.1088/0964-1726/14/4/029

Smart passive system based on magnetorheological damper

Sang-Won Cho[1], **Hyung-Jo Jung**[2] **and In-Won Lee**[3]

[1] The Boundary Layer Wind Tunnel Laboratory, Department of Civil and Environmental Engineering, The University of Western Ontario, London, ON, N6A 5B9, Canada
[2] Department of Civil and Environmental Engineering, Sejong University, 98 Gunja-dong, Gwangjin-Gu, Seoul 143-747, Korea
[3] Department of Civil and Environmental Engineering, Korea Advanced Institute of Science and Technology, 373-1 Guseong-dong, Daejeon 305-701, Korea

E-mail: swcho815@yahoo.co.kr, hjung@sejong.ac.kr and iwlee@kaist.ac.kr

Received 10 February 2003, in final form 23 May 2005
Published 29 June 2005
Online at stacks.iop.org/SMS/14/707

Abstract
Magnetorheological (MR) dampers are one of the most promising control devices for civil engineering applications to earthquake hazard mitigation, because they have many advantages such as small power requirement, reliability, and low price to manufacture. To reduce the responses of the controlled structure by using MR dampers, a control system including a power supply, controller, and sensors is needed. However, when a lot of MR dampers are applied to large-scale civil structures, such as cable-stayed bridges and high-rise buildings, the control system becomes complex. Thus, it is not easy to install and to maintain the MR damper-based control system.

In this paper, to resolve the above difficulties, a smart passive system is proposed, which is based on an MR damper system. The smart passive system consists of an MR damper and an electromagnetic induction (EMI) system that uses a permanent magnet and a coil. According to the Faraday law of induction, the EMI system that is attached to the MR damper produces electric energy. The produced energy is applied to the MR damper to vary the damping characteristics of the damper. Thus, the smart passive system does not require any power at all. Furthermore, the output of electric energy is proportional to input loads such as earthquakes, which means the smart passive system has adaptability by itself without any controller or corresponding sensors. Therefore, it is easy to build up and maintain the proposed smart passive system.

To verify the effectiveness of the proposed smart passive system, the performance is compared with that of the normal MR damper-based control system. The numerical results show that the smart passive system has comparable performance to the normal MR damper-based control system.

(Some figures in this article are in colour only in the electronic version)

1. Introduction

Magnetorheological (MR) dampers are one type of semi-active control devices, which use MR fluids to provide controllable damping forces. MR fluids consist of a suspension of iron particles in a carrier medium such as oil. Application of a magnetic field to the fluid causes the particles to align, and interparticle bonds increase the resistance of the fluid, turning the fluid into a semisolid (Weiss *et al* 1994, Ginder *et al* 1996). Since Spencer first introduced MR dampers to civil engineering applications in the mid-1990s, MR dampers have received considerable attention, because of their mechanical simplicity, high dynamic range, low operating power requirements, large force capacity, and environmental

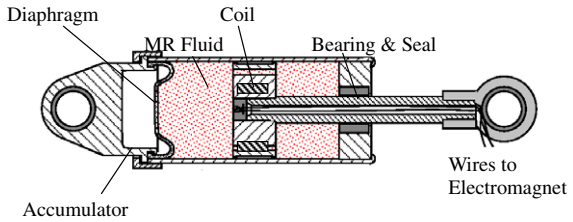

Figure 1. Schematic diagram of an MR damper (Dyke *et al* 1996a).

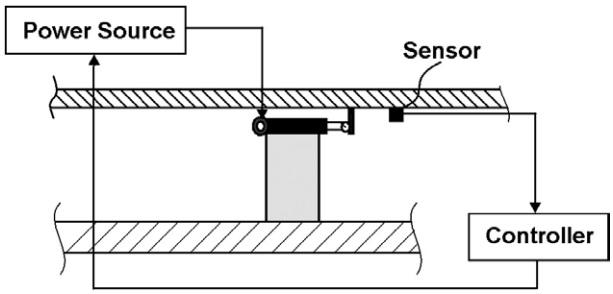

Figure 2. Schematic diagram of an MR damper-based control system.

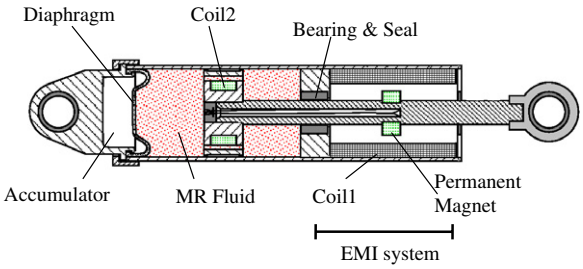

Figure 3. Schematic diagram of a smart passive system.

robustness (Kamath and Wereley 1997, Dyke and Spencer 1996, Ginder *et al* 1996, Spencer *et al* 1997a, Spencer and Sain 1997, Dyke *et al* 1998). In 2001, MR dampers was applied to the cable-stayed Dongting Lake Bridge in China and the Nihon-Kagaku-Miraikan building in Japan for reduction of responses of the structures, which are the world's first full-scale implementations in civil engineering structures (Spencer and Nagarajaiah 2003).

To reduce the responses of structures with MR dampers, a control system including power supply, controller, and sensors is required (Soong 1990). However, when a lot of MR dampers are used in a large-scale civil structure such as a cable-stayed bridge, the control system becomes complex: many MR dampers are used and then each MR damper must be connected to one or more power supplies and controllers. Also, many sensors are needed to measure structural responses. Thus, it is not easy to install and maintain an MR damper-based control system for a large-scale civil structure.

To resolve the above difficulties, this paper proposes a smart passive system that consists of an MR damper and an electromagnetic induction (EMI) system. An EMI system that comprises a permanent magnet and solenoid coils is attached to the MR damper. According to the Faraday law of induction (Reitz *et al* 1993, Marshall and Skitek 1990, Miner 1996), the EMI system changes the kinetic energy of the reciprocation motion of the MR damper to electric energy for the MR damper. Thus, the MR damper with EMI system is a passive system that does not require any power at all. Furthermore, the induced electric energy is proportional to external loads like earthquakes, which means that the smart passive system is adaptable to external loads by itself without any controller or corresponding sensors. General passive systems lack this adaptability whereas the MR damper with EMI system is a 'SMART' passive system to overcome shortcomings of general passive systems. These are important benefits of using the smart passive system.

An EMI system was adopted to control an engine mount of a vehicle (Korean patent 2000-004066), and to control an electrorheological (ER) damper (Japan patent 2-145337). Also, we got the Korean patent of the smart passive system for civil structures (Korean patent 2002-0061823). This paper focuses on civil engineering applications of the smart passive system. Through the numerical example, effectiveness and performance are evaluated and compared with those of a semi-active control system based on MR dampers.

2. Smart passive system

A prototype of MR damper is considered here to show the scheme of MR dampers, which was obtained for evaluation from the Lord Corporation and was used by Dyke *et al* (1996a). The damper is 21.5 cm long in its extended position, and the main cylinder is 3.8 cm in diameter. The main cylinder houses the piston, the electromagnet, an accumulator and 50 ml of MR fluid, and the damper has a ± 2.5 cm stroke. As shown in figure 1, the magnetic field produced in the device is generated by a small electromagnet in the piston head. The current for the electromagnet is supplied by a power supply such as a battery and regulated by a controller which determines control commands resulting in changes of damping characteristics of MR fluid. Thus, to reduce the structural responses, the MR damper needs a control system that consists of a power supply, a controller, and sensors as shown in figure 2. Although the MR damper-based control system in figure 2 seems to be simple, the MR damper-based control system becomes more complicated to build up and maintain when many MR dampers are used for civil engineering structures such as cable-stayed bridges and high-rise buildings.

To overcome previous disadvantages, in this paper, an electromagnetic induction (EMI) system is newly adopted to MR dampers. Figure 3 shows the MR damper with the EMI system that consists of a permanent magnet and coil1. The EMI system changes the kinetic energy of the reciprocation motion of the MR damper to electric energy according to the Faraday law of induction (Reitz *et al* 1993, Marshall and Skitek 1990, Miner 1996). The induced current in coil1 can be estimated by the Faraday law of induction as follows:

$$\varepsilon = -N \frac{\mathrm{d}\Phi_{\mathrm{B}}}{\mathrm{d}t} \tag{1}$$

where ε is the induced electromotive force (emf) that has the unit of volts (V), N is the number of turns of coil, and Φ_{B} is the magnetic flux. The negative sign in equation (1) is the

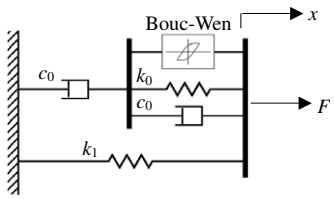

Figure 4. Simple mechanical model of the normal MR damper (Spencer *et al* 1997a).

direction of induced current. In equation (1), magnetic flux can be defined

$$\mathrm{d}\Phi_{\mathrm{B}} = \vec{A} \cdot \mathrm{d}\vec{B} = A\,\mathrm{d}B \cdot \cos\phi \tag{2}$$

where $\vec{A}$ is the area of cross section, $\vec{B}$ is the magnetic field, and ϕ is the angle between $\vec{A}$ and $\mathrm{d}\vec{B}$. Using equation (2), the Faraday law can be rewritten as follows:

$$\varepsilon = -N\,\frac{\mathrm{d}\Phi_{\mathrm{B}}}{\mathrm{d}t} = -N\,A\,\frac{\mathrm{d}B}{\mathrm{d}t}. \tag{3}$$

The Faraday law of induction states that the induced emf in a closed loop equals the negative of the time rate of change of magnetic flux through the loop. In other words, relative motions between coil1 and the permanent magnet cause a change of magnetic flux, which induces emf in the coils. Provided that a permanent magnet of 1.2 T is used in the EMI system for the prototype MR damper in figure 1, the maximum velocity of reciprocal motion of the MR damper is 9 cm s^{-1} (that is about the maximum velocity of the uncontrolled case of the following numerical example), and the turns of the coil are 900, then the time rate of change of magnetic field during the full stroke of 5 cm is 2.16 T s^{-1} and the resulting emf induced in the coil1 is about 2.54 V by the Faraday law. Considering that saturation of the MR effect begins in the prototype device when the applied voltage is 2.25 V, the maximum induced emf, 2.54 V, is enough to change the damping characteristics of the MR fluid. Of course, the amount of induced emf can be regulated by the turns of the coil or the intensity of the permanent magnet.

This induced electric energy is used at coil2 to make magnetic fields that solidify the MR fluid, which results in the change of damping characteristics of the MR damper. Thus, the MR damper with EMI system is a passive system that does not require any external power at all. Also, the MR damper with EMI system is capable of being adjusted to the vibrations of structures by itself without any controller, since fast relative motions between the permanent magnet and coil1 give high current in coil1 and slow relative motions give low current in coil1 according to the Faraday law. Therefore, the proposed MR damper with EMI system is a 'SMART' passive system whereas other passive systems lack this adaptability. These are most important features of using the smart passive system that can replace a conventional MR damper-based control system.

3. Analytical model

A simple mechanical model of a conventional MR damper is shown in figure 4. The equations governing the force f predicted by this model were given by Spencer *et al* (1997a) as follows:

$$\begin{aligned} f &= c_1\dot{y} + k_1(x - x_0) \\ \dot{z} &= -\gamma|\dot{x} - \dot{y}|z|z|^{n-1} - \beta(\dot{x} - \dot{y})|z|^n + A(\dot{x} - \dot{y}) \\ \dot{y} &= \frac{1}{(c_0 + c_1)}\{\alpha z + c_0\dot{x} + k_0(x - y)\}. \end{aligned} \tag{4}$$

To account for the dependence of the force on the voltage applied and the resulting magnetic current, Spencer *et al* (1997a) have suggested

$$\begin{aligned} \alpha(u) &= \alpha_a + \alpha_b u \\ c_1(u) &= c_{1a} + c_{1b}u \\ c_0(u) &= c_{0a} + c_{0b}u \end{aligned} \tag{5}$$

where u is given as the output of a first-order filter given by

$$\dot{u} = -\eta(u - v) \tag{6}$$

and v is the commanded voltage sent to the current driver, which is the emf induced by the EMI system.

The induced emf, v, is given by the Faraday law of induction in equation (6) assuming the ideal case without any magnetic leakage or interference. Thus, the amount of emf can be regulated by the turns of the coil with a fixed capacity of the permanent magnet. The appropriate number of coil turns should be determined for better performance of the smart passive system. In this study, the maximum response approach (Park *et al* 2003) is used to determine the number of coils by using parameters $\boldsymbol{S}_{\mathrm{a}}$ and $\boldsymbol{S}_{\mathrm{i}}$. $\boldsymbol{S}_{\mathrm{a}}$ is the summation of peak acceleration and $\boldsymbol{S}_{\mathrm{i}}$ the summation of peak inter-drift displacement at each floor, which are normalized by uncontrolled responses, respectively. The maximum response approach chooses the minimum of the envelope for summation of parameters. Figure 5(a) shows the variations of $\boldsymbol{S}_{\mathrm{a}}$ for each earthquake and figure 5(b) is the envelope of the maximum responses of figure 5(a). From figure 5(b), we can determine the optimal coil turns, which is the minimum point of the envelope denoted by the arrow. Figure 6 is similar to figure 5 except that it is for $\boldsymbol{S}_{\mathrm{i}}$. From the figures 5 and 6, two appropriate coil turns, 2.16×10^4 and 2.6×10^4 (turns m^{-1}), are determined. Finally, a smart passive system, designed for $\boldsymbol{S}_{\mathrm{a}}$, is designated $\mathrm{EMI}_{\mathrm{ac}}$ and the other smart passive system, designed for $\boldsymbol{S}_{\mathrm{i}}$, is called $\mathrm{EMI}_{\mathrm{dr}}$.

For the comparison of the performance, a normal MR damper system using the clipped optimal controller (Dyke *et al* 1996a, 1996b) is considered. This strategy is as follows. First, an 'ideal' active control device is assumed, and an appropriate primary controller for this active device is designed. Then a secondary bang–bang type controller causes the MR fluid damper to generate the desired active control force, so long as this force is dissipative. In this study, an H_2/LQG control design is adopted as the primary controller. The ground excitation is taken to be a stationary white noise, and an infinite horizon performance index is chosen that weights appropriate parameters of the structure, i.e.

$$J = \lim_{\tau\to\infty}\frac{1}{\tau}E\left[\int_0^{\tau}\{\mathbf{z}^{\mathrm{T}}\mathbf{Q}\mathbf{z} + \mathbf{f}^{\mathrm{T}}\mathbf{R}\mathbf{f}\}\,\mathrm{d}t\right] \tag{7}$$

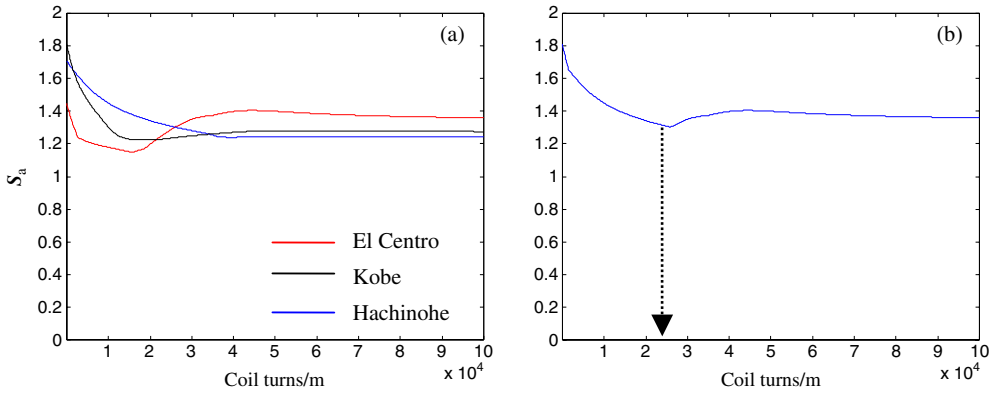

Figure 5. Design of smart passive system with S_a under three earthquakes. (a) Variations of S_a. (b) Envelope of maximum responses of (a).

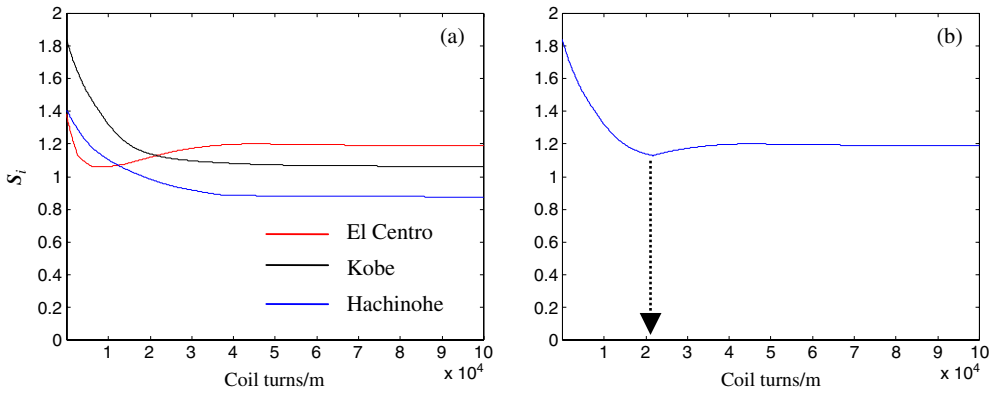

Figure 6. Design of smart passive system with S_i under three earthquakes. (a) Variations of S_i. (b) Envelope of maximum responses of (a).

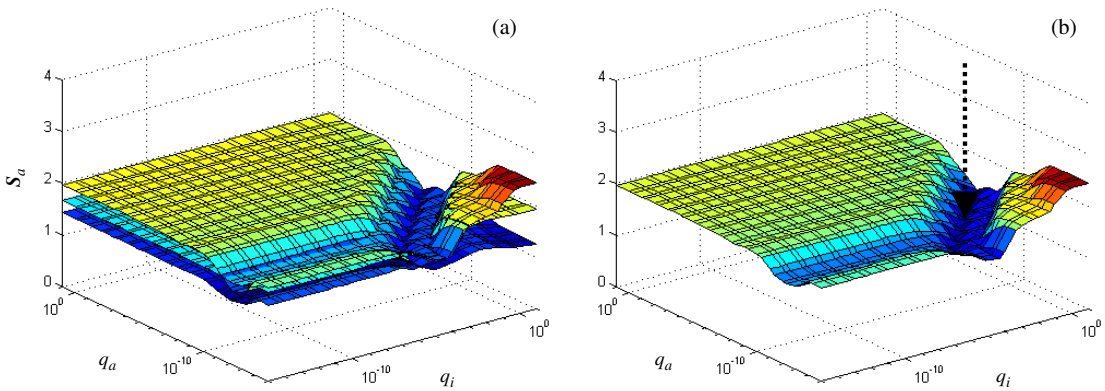

Figure 7. Design of the clipped-optimal controller with S_a under three earthquakes. (a) Variations of S_a. (b) Envelope of maximum responses of (a).

where **R** is an identity matrix, and **Q** is the response weighting matrix. The weighting parameters are as in equation (8).

$$\mathbf{Q} = \begin{bmatrix} q_a \mathbf{I}_{3\times 3} & 0 \\ 0 & q_i \mathbf{I}_{3\times 3} \end{bmatrix} \tag{8}$$

where q_a and q_i weight the accelerations and the inter-story drifts at each floor, respectively. To determine the weighting parameters q_a and q_i, the maximum response approach is used as in the smart passive system for three earthquakes. Figure 7(a) shows the variations of S_a for increasing weighting parameters in a three-dimensional plot. Each surface corresponds to the variation of S_a for each earthquake. Figure 7(b) is the envelope of the maximum response of figure 7(a). From figure 7(b), we can determine the appropriate weighting parameters, which is the minimum point of the envelope denoted by the arrow. Figure 8 is similar to figure 7 except that it is for S_i. Two sets of appropriate weighting parameters, $q_a = 5.0 \times 10^{-13}$, $q_i = 1.0 \times 10^{-5}$ for S_a and $q_a = 5.0 \times 10^{-15}$, $q_i = 5.0 \times 10^{-6}$ for S_i, are determined from figures 7 and 8. The clipped-optimal controller, designed for S_a, with weighting parameters q_a and q_i, is designated CLO_{ac}, and the other, designed for S_i, is called CLO_{dr}.

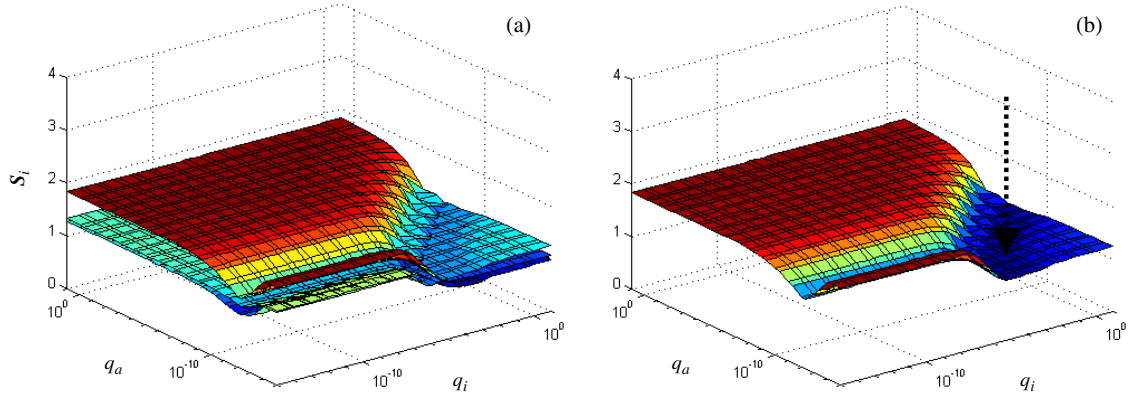

Figure 8. Design of the clipped-optimal controller with S_i under three earthquakes. (a) Variations of S_i. (b) Envelope of maximum responses of (a).

4. Numerical example

The performance of the smart passive system is now evaluated through simulations. A model of a three-story building configured with a single MR damper is considered here for direct comparisons with the normal MR damper, which is the exact one used by Dyke *et al* (1996a). The MR damper is rigidly connected between the ground and the first floor of the structure. A schematic diagram of the MR damper implementation is shown in figure 9.

The governing equations of the structure are given by

$$\dot{z} = Az + Bf + E\ddot{x}_g \tag{9}$$

where $\ddot{x}_g$ is a one-dimensional ground acceleration, f is the measured force generated between the structure and the MR damper, z is the state vector, and

$$A = \begin{bmatrix} 0 & I \\ -M^{-1}K & -M^{-1}C \end{bmatrix}, \qquad B = \begin{bmatrix} 0 \\ M^{-1}\Gamma \end{bmatrix},$$

$$E = -\begin{bmatrix} 0 \\ \Lambda \end{bmatrix} \qquad M = \begin{bmatrix} 98.3 & 0 & 0 \\ 0 & 98.3 & 0 \\ 0 & 0 & 98.3 \end{bmatrix} \text{kg},$$

$$C = \begin{bmatrix} 175 & -50 & 0 \\ -50 & 100 & -50 \\ 0 & -50 & 50 \end{bmatrix} \text{N s m}^{-1}$$

$$K = 10^5 \begin{bmatrix} 12.0 & -6.84 & 0 \\ -6.84 & 13.7 & -6.84 \\ 0 & -6.84 & 6.84 \end{bmatrix} \text{N m}^{-1},$$

$$\Gamma = \begin{bmatrix} -1 \\ 0 \\ 0 \end{bmatrix}, \qquad \Lambda = \begin{bmatrix} 1 \\ 1 \\ 1 \end{bmatrix}. \tag{10}$$

To verify the effectiveness of the proposed smart passive system, a set of simulations is performed for the four historical earthquakes of El Centro, Hachinohe, Kobe, and Northridge. The Northridge earthquake is not considered in the designing phase, but is included here to check the validation of the design of the smart passive system and the clipped-optimal controller. Simulation results of the proposed smart passive system are compared to those of the normal MR damper system using the clipped optimal controller by evaluation criteria based on

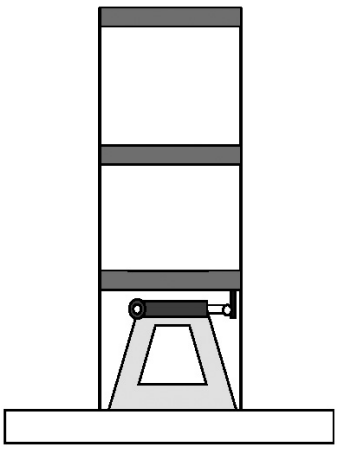

Figure 9. Schematic diagram of an MR damper implementation (Dyke *et al* 1996a).

those used in the second generation linear control problem for buildings (Spencer *et al* 1997b). The first evaluation criterion is a measure of the normalized peak floor accelerations, given by

$$J_1 = \max_{t,\,i}\left(\frac{|\ddot{x}_{ai}(t)|}{\ddot{x}_a^{\max}}\right) \tag{11}$$

where the absolute accelerations of the ith floor, $\ddot{x}_{ai}(t)$, are normalized by the peak uncontrolled floor acceleration, denoted $\ddot{x}_a^{\max}(t)$.

The second evaluation criterion is a measure of the reduction in the inter-story drift. The maximum of the normalized inter-story drift is

$$J_2 = \max_{t,\,i}\left(\frac{|d_i(t)|}{d_n^{\max}}\right) \tag{12}$$

where $d_i(t)$ is the inter-story drift of the above ground floors over the response history, and $d_n^{\max}$ denotes the normalized peak inter-story drift in the uncontrolled response.

Representative responses of the smart passive system to four earthquakes are shown in graphs. Figure 10 shows the velocities at the first floor where the MR damper is attached and the voltages induced by the smart passive system for

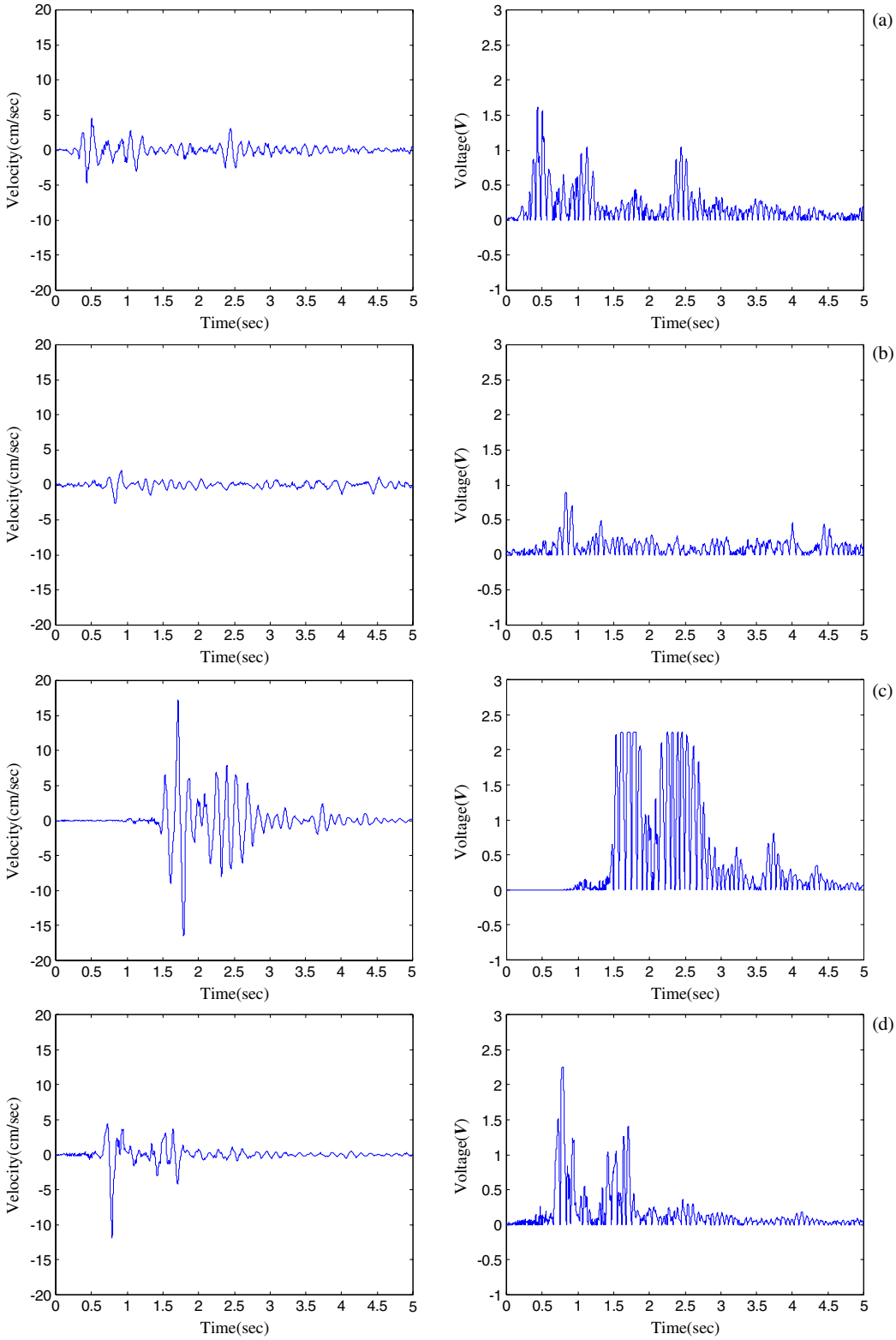

Figure 10. Velocities and induced voltages under various earthquakes. (a) El Centro earthquake. (b) Hachinohe earthquake. (c) Kobe earthquake. (d) Northridge earthquake.

each earthquake. For moderate earthquakes (El Centro and Hachinohe) the velocity of the first floor is smaller than that of severe earthquakes (Kobe and Northridge), with the consequence that the voltage induced by the EMI system is lower according to the Faraday law of induction. Also, it can be seen that the higher voltage is induced for severe earthquakes. The maximum induced voltage is 1.6 V, 0.9 V, 2.25 V, and 2.25 V for El Centro, Hachinohe, Kobe, and

Table 1. Normalized peak absolute accelerations and inter-story drifts.

Story	CLO_{ac}	CLO_{dr}	EMI_{ac}	EMI_{dr}	CLO_{ac}	CLO_{dr}	EMI_{ac}	EMI_{dr}
	Accelerations							
	El Centro (0.3495)[a]				Hachinohe (0.2294)			
1st	0.499	0.551	0.355	0.340	0.492	0.515	0.372	0.377
2nd	0.354	0.433	0.436	0.396	0.431	0.520	0.526	0.530
3rd	0.441	0.473	0.512	0.492	0.384	0.465	0.404	0.423
	Kobe (0.8337)				Northridge (0.8428)			
1st	0.370	0.429	0.367	0.345	0.897	0.881	0.568	0.568
2nd	0.494	0.493	0.484	0.485	0.587	0.554	0.612	0.586
3rd	0.410	0.384	0.387	0.393	0.815	0.800	0.725	0.738
	Inter-story drifts							
	El Centro (0.3495)				Hachinohe (0.2294)			
1st	0.228	0.212	0.168	0.180	0.295	0.243	0.178	0.194
2nd	0.423	0.448	0.476	0.457	0.289	0.319	0.357	0.355
3rd	0.441	0.473	0.512	0.492	0.384	0.465	0.404	0.423
	Kobe (0.8337)				Northridge (0.8428)			
1st	0.348	0.308	0.293	0.301	0.563	0.473	0.359	0.382
2nd	0.456	0.442	0.428	0.435	0.859	0.846	0.827	0.835
3rd	0.410	0.384	0.387	0.393	0.815	0.800	0.725	0.738

[a] ( ) is peak ground acceleration (g).

Table 2. Percentage increment compared to the better clipped-optimal controller.

Story	CLO_{ac}	CLO_{dr}	EMI_{ac}	EMI_{dr}	CLO_{ac}	CLO_{dr}	EMI_{ac}	EMI_{dr}
	Accelerations							
	El Centro (0.3495)				Hachinohe (0.2294)			
1st	0	10.4	−28.8[a]	−31.9	0	4.7	−24.4	−23.4
2nd	0	22.1	23.1	11.7	0	20.5	22.0	22.9
3rd	0	7.3	16.0	11.5	0	21.4	5.4	10.4
	Kobe (0.8337)				Northridge (0.8428)			
1st	0	14.2	−0.7	−6.6	1.8	0	−35.5	−35.5
2nd	0.16	0	−1.8	−1.5	6.0	0	10.5	5.8
3rd	6.8	0	0.9	2.4	1.9	0	−9.4	−7.8
	Inter-story drifts							
	El Centro (0.3495)				Hachinohe (0.2294)			
1st	7.2	0	−20.6	−15.3	21.5	0	−26.7	−20.4
2nd	0	5.9	12.4	8.1	0	10.4	23.5	22.8
3rd	0	7.3	16.0	11.5	0	21.4	5.4	10.4
	Kobe (0.8337)				Northridge (0.8428)			
1st	12.8	0	−5.0	−2.5	19.0	0	−24.1	−19.2
2nd	3.2	0	−3.2	−1.6	1.5	0	−2.2	−1.3
3rd	6.8	0	0.9	2.4	1.9	0	−9.4	−7.8

[a] Minus means reduction.

Northridge earthquakes, respectively, which is enough voltage to be able to operate the MR damper. It should be noted that the induced voltage is restricted within 2.25 V for the capacity of the MR damper, which is the identical condition with the clipped-optimal controller. However, the induced voltage is continuously varying whereas the command voltage of the clipped-optimal controller takes on values of either zero or the maximum value.

Figure 11 shows the values for the peak acceleration and peak inter-story drift normalized by uncontrolled responses,

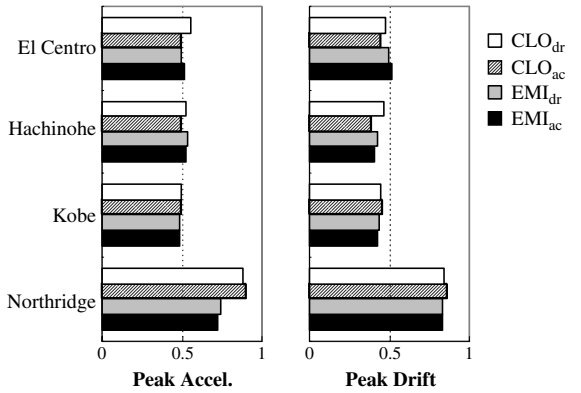

Figure 11. Normalized peak acceleration and inter-story drift.

where it can be seen that the smart passive system performs well over the entire suite of earthquakes considered. The reductions in peak acceleration and drift are comparable to those of the clipped-optimal controller—both giving as much as nearly 50% decrease compared to the uncontrolled responses, except the Northridge earthquake. Although the smart passive system and the clipped-optimal controller are designed under the three earthquakes except the Northridge earthquake, both achieve reductions in the peak acceleration and inter-story drift for the Northridge earthquake.

Table 1 shows the accelerations and the inter-story drifts at each floor for four cases of two categories (i.e., EMI_{ac}, EMI_{dr}, CLO_{ac}, and CLO_{dr}) normalized by each uncontrolled response, respectively. Table 2 reports the percentage response reduction (−) or increase (+) compared to the better clipped-optimal controller. In tables 1 and 2, the colored cells are the minimum value among four cases at each floor. In the table 2, the clipped-optimal controllers achieve more reduction over the smart passive systems for the moderate earthquakes such as El Centro and Hachinohe, except that the smart passive systems give a minimum value at the first floor. For the severe earthquakes such as Kobe and Northridge, however, the performances of the smart passive system are better than those of the clipped-optimal controller, giving 35.5% and 24.1% additional decreases in maximum in the peak acceleration and inter-story drift, respectively, compared to the better clipped-optimal controller. Though the smart passive system fails to achieve more reductions over the clipped-optimal controller for the moderate earthquakes, it has comparable performance to the clipped-optimal controller without the power source, controller, and sensors. This is the important benefit of using the smart passive system.

5. Concluding remarks

This paper has proposed a smart passive system for a civil engineering application. The smart passive system consists of an EMI system and MR damper. According to the Faraday law of induction, the EMI system generates induced voltages that can supply electricity and control commands to the MR damper, replacing a normal control system such as a power supply, a controller, and sensors.

To investigate the achievable capabilities of the smart passive system, two systems were designed. Then, the effectivenesses of performance are evaluated, and compared with those of a normal MR damper system. In comparing both systems, it was observed that for a moderate earthquake such as El Centro and Hachinohe the smart passive system showed comparable performance to the normal MR damper system. For the severe earthquakes such as Kobe and Northridge, the smart passive system shows the better performance, giving 35.5% and 24.1% additional maximum decreases in the peak acceleration and inter-story drift, respectively.

In addition to the comparable performance, the proposed smart passive system has the simple structure without any power supply, controller, and sensors and has adaptability to external loads by itself. These are important benefits of using the smart passive system.

References

Dyke S J and Spencer B F Jr 1996 Seismic response control using multiple MR dampers *Proc., 2nd Int. Workshop on Structural Control* (Hong Kong: Hong Kong University of Science and Technology Research Center) pp 163–73

Dyke S J, Spencer B F Jr, Sain M K and Carlson J D 1996a Modeling and control of magnetorheological dampers for seismic response reduction *Smart Mater. Struct.* **5** 565–75

Dyke S J, Spencer B F Jr, Sain M K and Carlson J D 1996b Seismic response reduction using magnetorheological dampers *Proc. IFAC World Congr. (San Francisco, CA, June–July, 1996)*

Dyke S J, Spencer B F Jr, Sain M K and Carlson J D 1998 An experimental study of MR dampers for seismic protection *Smart Mater. Struct.* **7** 693–703 (Special issue on Large Civil Structures)

Ginder J M, Davis L C and Elie L D 1996 Rheology of magnetorheological fluids: models and measurements *Int. J. Mod. Phys.* B **10** 3293–303

Kamath G M and Wereley N M 1997 A nonlinear viscoelastic-plastic model for electrorheological fluids *Smart Mater. Struct.* **6** 351–9

Marshall S V and Skitek G G 1990 *Electromagnetic Concepts and Applications* (Englewoods Cliffs, NJ: Prentice-Hall)

Miner G F 1996 *Lines and Electromagnetic Fields for Engineers* (Oxford: Oxford University Press)

Park K S, Jung H J and Lee I W 2003 Hybrid control strategy for seismic protection of a benchmark cable-stayed bridge *Eng. Struct.* **25** 405–17

Reitz J R, Milford F J and Christy R W 1993 *Foundations of Electromagnetic Theory* (Reading, MA: Addison-Wesley)

Soong T T 1990 *Active Structural Control: Theory and Practice* (Essex: Longman Scientific and Technical)

Spencer B F Jr, Dyke S J, Sain M K and Carlson J D 1997a Phenomenological model of a magnetorheological damper *J. Eng. Mech., ASCE* **123** 230–8

Spencer B F Jr, Dyke S J, Sain M K and Carlson J D 1997b Benchmark problems in structural control—part I: active mass driver system *Proc. ASCE Structures Congr. XV* (New York: ASCE) pp 1265–9

Spencer B F Jr and Nagarajaiah S 2003 State of the art of structural control *J. Struct. Eng., ASCE* **129** 845–56

Spencer B F Jr and Sain M K 1997 Controlling buildings: a new frontier in feedback *IEEE Control Syst. Mag.* **17** 19–35 (Special issue on Emerging Technologies, Guest ed T Samad)

Weiss K D, Carlson J D and Nixon D A 1994 Viscoelastic properties of magneto- and electro-rheological fluids *J. Intell. Mater. Syst. Struct.* **5** 772–5